

# Contact Area Effects on Superficial and Deep Pain Threshold for Service Robot Safety Design using a Pain-sensing System

## - Development of a Human-inspired Pain-sensing System -

### 人共存ロボットの安全設計に向けたPain-sensingシステムの開発 - 人体衝突時の接触面積と表在痛／深部痛しきい値の関係 -

Tanyaporn Pungrasmi  
ブングラサミー タンヤポン

Yusaku Shimaoka  
島岡 優策

Tamao Okamoto  
岡本 球夫

Ryoji Watanabe  
渡邊 龍司

#### Abstract

Logistic and service robots are now increasingly collaborating with humans in a public environment; hence, there is a necessity for a safety evaluation. Therefore, this study focuses on pressure pain thresholds that humans feel when in contact with the robots. The pain threshold was measured in the forearms of fifteen subjects using four different probe areas: 0.5, 2.0, 3.6, and 5.8 cm<sup>2</sup>. The same experiment was conducted using the proposed pain-sensing system. The obtained results were compared with those obtained from the subjects to validate the proposed system. This system imitates the sensing location of pain receptors in the human skin (superficial somatic pain) and skeletal muscle (deep somatic pain) by placing a pressure sensor in each layer. At the pain threshold point, maximum pressure in superficial sensors for a contact area probe of 0.5 cm<sup>2</sup> was at the highest; no considerable differences were observed in the remaining probes when compared with the 0.5 cm<sup>2</sup> probe. Meanwhile, the maximum pressure in deep sensor for every probe were considerably equal. By using this system, it is possible to measure pressure distribution in two layers to predict the pain in humans while being in contact by different area objects in contact area. The results of the relationship between contact area and pain can be used to design the safety protocol in logistic or service robot safety design industries.

#### 1. Introduction

As there have been considerable developments in the field of logistic and service robotics, it is now possible to make them interact with humans. However, as the possibility of contact between a human and a robot (Fig. 1) is increasing, a safety evaluation is required to minimize the risk of human injury.

Further, it is important to ensure the safety of these types of robots, which provide various services to humans while sharing the same space with them. Hence, contact limits using “pain” as a mechanical threshold was studied by conducting pressure pain tolerance and pressure pain threshold (PPT) experiments with

humans [1]–[3] to measure the force or pressure from a probe in contact with the human skin. However, the existing studies did not consider the relationship between contact area and pain.

PPT experiments using probe areas of 0.5, 1.0, 2.0 cm<sup>2</sup> [4], 0.25, and 0.75 cm<sup>2</sup> [5], and pressure pain tolerance experiments using stimulus area of 0.78 and 5.3 cm<sup>2</sup> [6] were conducted. In these experiments, average pressures were calculated using force and contact area. However, the correlation between pain and contact area is still unclear. Our study tries to address this matter by focusing on pressure distribution considering contact area. To investigate the mechanism of pain, we developed a human-inspired pain-sensing system [7] (refer to Fig. 6). This system imitates the sensing location of mechanical nociceptors in the human skin (superficial somatic pain) and skeletal muscle (deep somatic pain) (refer to Fig. 2). It consisted of an artificial skin layer, adipose tissue combined with muscle layer, bone



Fig. 1 Service robot moving interactively with humans in the same environment

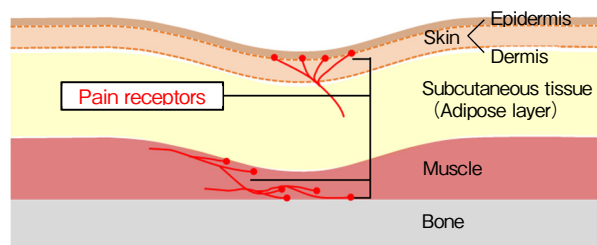


Fig. 2 Mechanism of pain sensation in human arm

layer, and two flexible pressure array sensors placed under each layer excluding the bone. This was done to evaluate the pressure distribution where the pain receptors exist [8] (refer to Fig. 3). In Section 2.5, we will validate and verify the mechanical properties of the pain-sensing dummy by comparing it with experiment results from the subjects.

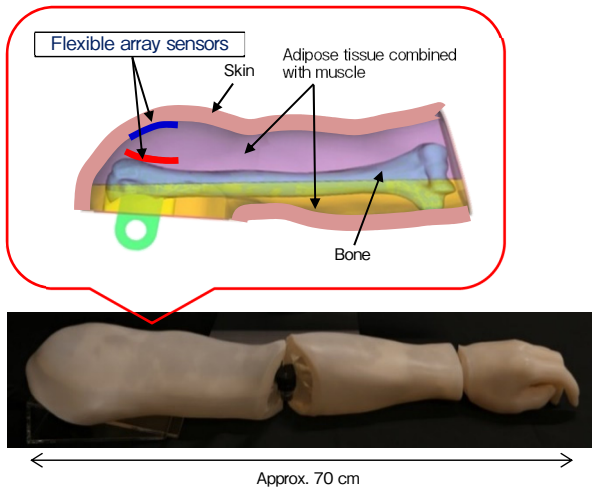


Fig. 3 Upper arm human-inspired pain-sensing dummy structure that consisted of artificial skin layer, adipose tissue combined with muscle layer, bone layer, and two flexible pressure array sensors placed under skin layer and top of bone layer around deltoid muscle area

Pressure sensors in the range 34.5 kPa–3 MPa were placed in between the abovementioned layers. A sampling rate of 500 Hz or above and spatial resolution of 2.54 mm × 2.54 mm, were selected for the sensors, respectively, with sensing area of 30.5 mm × 40.6 mm.

In the present study, the relationship between pain and contact area when humans are in contact with collaborative robots was evaluated by performing pain threshold experiments with human volunteers. Furthermore, the biofidelity of the pain-sensing system was verified using the force and displacement relationship obtained from the experiment. Finally, the pain mechanism was determined by analyzing the relationship between contact area and pressure distribution of superficial and deep sensors.

## 2. Materials and methods

### 2.1 Subjects

Fifteen healthy adult Japanese male subjects aged between 30 and 50 years, BMI between 20 and 25 kg/m<sup>2</sup>, and height between 165 and 175 cm participated in the study. The subjects

were screened to exclude conditions that could affect pain perception, such as past operation in their non-dominant arm. All subjects were pain-free and none had taken any analgesic or sedative medication for a minimum of 48 h prior to the test session. The study protocol was approved by the health care ethics committee of Panasonic Corporation. All subjects were paid for participating and gave written informed consent.

### 2.2 Indentation system

The experiment was conducted with indentation system for mechanical stimuli, which is able to measure a maximum force of 500 N, with error <0.25 % ( $\pm 1.2$  N) from the measurement value, and maximum probe displacement of 120 mm with error <0.09 % ( $\pm 0.1$  mm) from the measurement value, which has been explained in our previous study [7]. To measure samples from any direction, it was designed using a joint that can be rotated  $\pm 45^\circ$  in horizontal and vertical directions (refer to Fig. 5 (a)). Furthermore, it is possible to adjust the initial position along both horizontal and vertical directions using the linear slide attached within this system. The system sampling rate was 1000 Hz that was enough for the measurement.

### 2.3 Contact probe

To study the effect of probe area while in contact with human, an experiment was conducted using four square probes with dimensions of 7 mm × 7 mm (S7), 14 mm × 14 mm (S14), 19 mm × 19 mm (S19), and 24 mm × 24 mm (S24) (refer to Fig. 4). We rounded the corners and edges by a radius of 2 mm to reduce the sharpness [3].

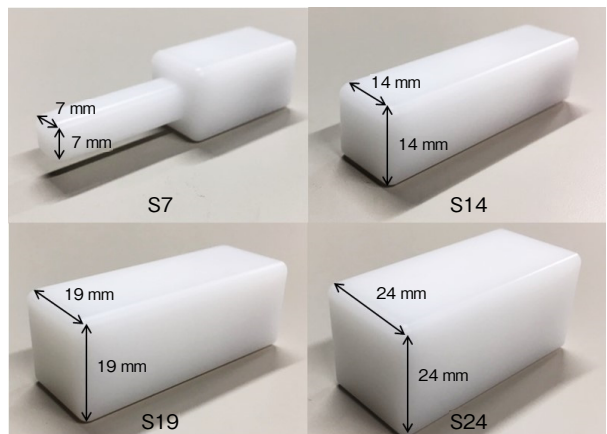


Fig. 4 Tested four square contact probe

### 2.4 Procedure

The experiment was 2 h long for each subject and was

conducted in a quiet room during the daytime (between 10 am and 5 pm). The experimental procedures were made familiar to all the subjects; they were trained until they understood all the procedures. Hence, they were able to follow the instructions before the experiment started. The point of measurement was set on a non-dominant forearm muscle (refer to Fig. 5(b)).

A semi-automatic indentation system was used in the experiment. The initial position of the probe was adjusted manually, and during the measurement, the probe was moved toward the body by 1 mm at a speed of 2 mm/s, which is the quasi-static speed, and stopped for 2 s. This was done repeatedly until the subjects started to feel pain; they were requested to immediately press the stop button themselves. Then, the probe returned to the initial position. A vacuum cushion was used to stabilize the arm during the experiment (refer to Fig. 5 (b)).

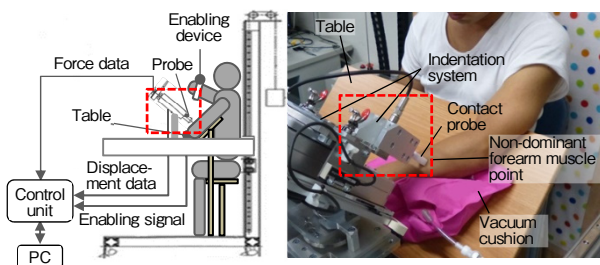


Fig. 5 Indentation system schematic (a), Indentation system at non-dominant forearm muscle point using S14 probe during the experiment (b)

This experiment was repeated three times with a minimum resting interval of 45 s in between each experiment, which was required to prevent desensitization from a repeated pressure [9]. The measurement point was specified at the forearm muscle point according to the previous study [3]. The force and displacement data were recorded during the measurement.

## 2.5 Validation and verification of pain-sensing dummy

In this study, we had developed full arm dummy for a human-inspired pain-sensing system that consists of artificial skin, adipose tissue combined with muscle, and bone according to Japanese adult average data from AIST (National Institute of Advanced Industrial Science and Technology) [10] with a skin thickness of 2 mm [11] [12]. As for the mechanical characteristic of each part, based on the previous studies of human arm, we defined the Young's modulus of the skin and muscle to be around 100 kPa [13] and 35 kPa [14]–[16], respectively. Further, we defined the compressive loading of bone to be around 160 MPa [17]. This dummy simulated the

nociceptor (pain receptor) function of the human arm by placing two flexible pressure array sensors under each layer excluding the bone [7].

We verified the biofidelity of our human arm dummy (refer to Fig. 6) by repeating the same experiment procedure with using this dummy, and then the results were compared using the relationship between force and displacement from fifteen subjects. The force and displacement curve for the dummy is in between the minimum and maximum displacement curves obtained from the subjects (refer to Fig. 7). This experiment revealed that this dummy turned out to have mechanically similar properties to the human arm. Together with the fact that the sensor is embedded in an anatomically correct manner, this dummy has biofidelity. As a result, the dummy was in a satisfied range compared with pain threshold from the subjects.

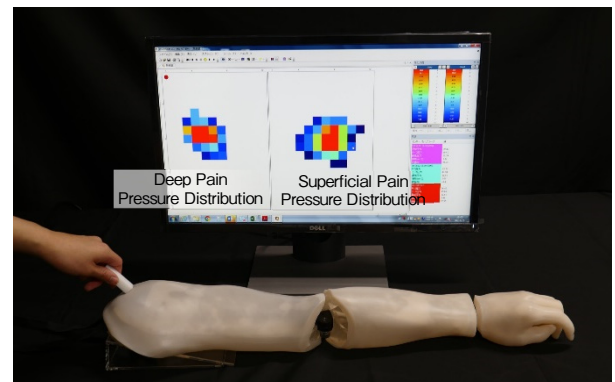


Fig. 6 Arm part of pain-sensing system showing pressure distribution at superficial layer sensor and deep layer sensor around deltoid muscle area

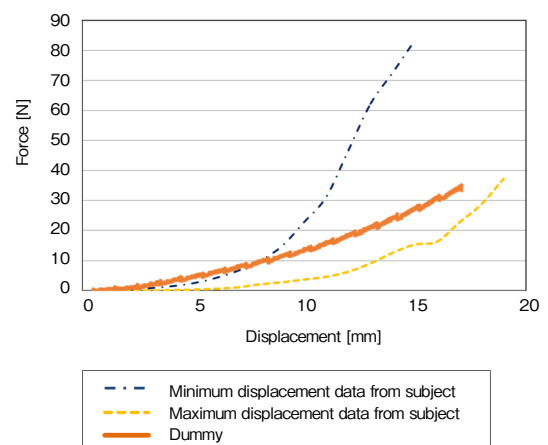


Fig. 7 Relationship between force [N] and displacement [mm] of maximum and minimum displacement data from 15 subjects and pain-sensing dummy at non-dominant forearm point

### 3. Results

#### 3.1 Pain threshold from subjects

The average of the pain thresholds obtained using the indentation system for the non-dominant forearm muscle point [3] for every subject using four different probes in the contact area are shown in Fig. 8. For probes S7, S14, S19, and S24, the average pain threshold from 15 subjects with three repeated measurements are  $15.9 \pm 2.1$  N,  $21.7 \pm 2.5$  N,  $27.8 \pm 2.6$  N, and  $33.9 \pm 3.9$  N ( $\pm SD$ ) respectively. This graph clearly showed that pain thresholds for each contact area are different. Therefore, it is necessary to evaluate the pain threshold using pressure distribution rather than the average force.

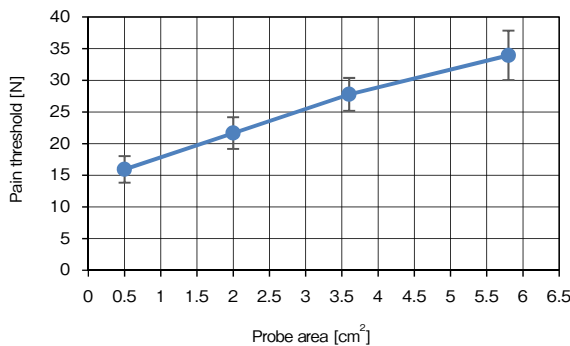


Fig. 8 Graph of average and SD of relationship between pain threshold and probe area: S7 ( $0.5 \text{ cm}^2$ ), S14 ( $2.0 \text{ cm}^2$ ), S19 ( $3.6 \text{ cm}^2$ ), and S24 ( $5.8 \text{ cm}^2$ )

#### 3.2 Pain threshold pressure distribution from pain-sensing system

The experiment was conducted with the subjects and then the pain-sensing system to obtain the pressure distribution. According to ISO/TS 15066 Robot and Robotic devices – Collaborative Robots [18], the recommendation of biomechanical limits for each body region, while humans are in contact with the robot, is defined by the maximum permissible pressure indicated by the maximum pressure during impact. Thus, to analyze the pain threshold pressure distribution, we used maximum pressure values obtained using this sensing system. Maximum pressure from superficial pressure and deep pressure are displayed in Fig. 9.

Experiment results revealed that at the pain threshold point, the maximum pressure in a superficial sensor for S7 probe was the highest, while in S14, S19, and S24, there was no considerable difference ( $\leq 20\%$ ) compared with the S7 probe. Meanwhile, the maximum pressure in deep sensor for every probes were considerably equivalent ( $\leq 20\%$ ) compared with

the S7 probe.

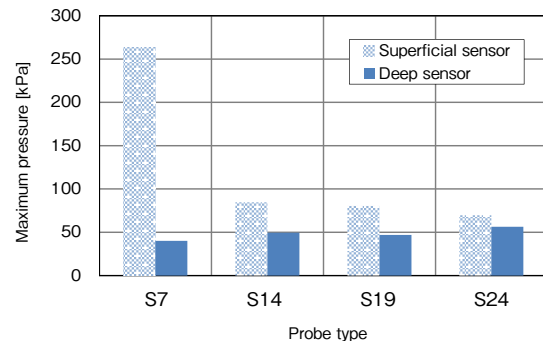


Fig. 9 Maximum pressure in superficial sensor and deep sensor during compression at pain-sensing dummy with  $7 \text{ mm} \times 7 \text{ mm}$  (S7),  $14 \text{ mm} \times 14 \text{ mm}$  (S14),  $19 \text{ mm} \times 19 \text{ mm}$  (S19), and  $24 \text{ mm} \times 24 \text{ mm}$  (S24) square probe at the same force with

### 4. Discussion

The contribution of this paper consists of four parts. First, we developed a human-inspired pain-sensing system, which imitates the sensing location of mechanical nociceptors in human skin and skeletal muscle.

Second, we conducted the pain threshold experiment with fifteen subjects in the forearms using four different probe areas:  $0.5$ ,  $2.0$ ,  $3.6$ , and  $5.8 \text{ cm}^2$  and collected force and displacement data from our indentation system. Pain threshold with different probe sizes from subjects showed different results. The S7 probe that has the smallest contact area has the lowest average pain threshold; further, the S24 probe that has the biggest contact area has the highest average pain threshold. These might be explained by the pressure distribution results obtained using the pain-sensing system; the pain thresholds are not related to the magnitude of the external force on the skin; however, they are more related with the pressure distribution in superficial layer and deep layer, as suggested in [19]–[22]. These studies discussed how pressing using cuff algometry affects the muscle pain more than cutaneous pain (superficial pain). However, these studies did not discuss the exact contact area that might cause both muscle and cutaneous pain.

Third, we evaluated the biofidelity of our developed human arm dummy by conducting a pain threshold experiment, where the force and displacement curve for the dummy is in between the minimum and maximum curves obtained from the subjects with the compression speed of  $2 \text{ mm/s}$ . Therefore, this pain-sensing dummy is considered as a good pressure measurement system when the human arm is in contact with the

robot at the quasi-static speed.

Finally, we collected pressure distribution from the pain-sensing system using the same force pain threshold obtained from the pain threshold experiment. We found that the pain threshold for the forearm muscle, while using the probe with surface area equal or larger than  $14 \text{ mm} \times 14 \text{ mm}$  ( $2.0 \text{ cm}^2$ ), might result in deep pain owing to similar maximum pressure obtained from deep sensors at the pain-onset thresholds. In probe S7 ( $0.5 \text{ cm}^2$ ) where superficial maximum pressure is the highest and the deep maximum pressure can be considered the lowest compared with the bigger probes, the pain might originate from either superficial layer or deep layer or from the summation of both layers (refer to Fig. 10).

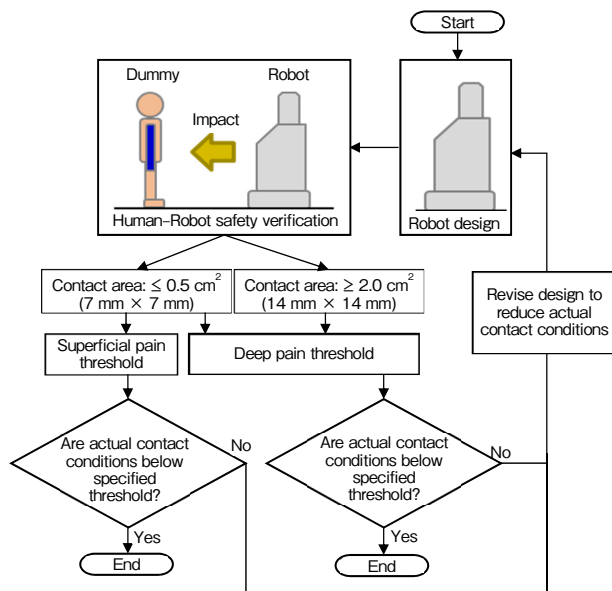


Fig. 10 Our hypothesis of the relationship between contact area and 2 types of pain (superficial and deep pain) according to the results from pain-sensing system with example of flowchart for application using pain threshold as a human-robot safety limit

Furthermore, with these results, it might be possible to conclude that by using maximum pressure at probe with surface area equal or larger than  $2.0 \text{ cm}^2$ , the contact area has less effect on the superficial pain threshold.

This study is our second step to measure superficial and deep pain to ensure the mechanical safety of service and logistic robots.

In the future, we are planning to verify human superficial and deep pain threshold by conducting anesthetized pain threshold experiment on a human to see whether our assumption of relationship between two types of pain (superficial and deep

pain) and contact area are accurate. In this experiment we have conducted the experiment with only quasi-static condition; however, in real contact condition, both quasi-static and dynamic conditions are required. Thus, the experiment in dynamic condition is also necessary. Then, we will correlate the pressure in proposed method with the pain recognized by humans using the pain threshold measurement system. Our main goal is to obtain the satisfying accuracy of the system so that it can be used to predict mechanical pain incident supporting safety design in logistic and service robot industries.

## 5. Conclusion

The present study showed that pressure distribution obtained from superficial and deep sensors could be used to determine the mechanism of pain.

The highest pain threshold assessed by the subjects was observed in the pain-onset area, which is the pain at the starting point. The assessments of pain threshold also represent useful data for the safety of human-robot interaction in terms of allowable robot contact area and force. Moreover, the pain-sensing system's maximum pressure values also express data in terms of robot contact area and pressure threshold in the superficial and deep layers, which can be applied in terms of acceptable maximum robot contact pressure for each layer in any contact area.

We believe that this dummy will be useful in logistic and service robotics. Further, it can also be applied to collaborative robots with varied design parameters, such as shape, weight, compliance, and speed, using our pressure threshold for each layer.

This research was funded by ImPACT (Impulsing Paradigm Change through Disruptive Technologies) Program of Council for Science, Technology and Innovation (Cabinet Office, Government of Japan).

## References

- [1] Y. Yoji et al., "Evaluation of Pain Tolerance Based on a Biomechanical Method for Human-Robot Coexistence," Trans. Jpn. Soc. Mech. Eng. C, vol.63, no.612, pp.238–243, 1997. (Japanese).
- [2] S. Tsuyoshi et al., "Measurement of Human Pain Tolerance to Mechanical Stimulus of Human-collaborative Robots," NIIS-SRR. no.33, 2005. (Japanese).

- [3] A. Muttray, et al., "Collaborative Robots – Determination of pain sensitivity at the human-machine-interface," Universitätsmedizin, Institut für Arbeits-, Sozial und Umweltmedizin, Mainz. Project FP0317 Final report, 2014.
- [4] R.M. Slugg et al., "Response of cutaneous A- and C-fiber nociceptors in the monkey to controlled-force stimuli," *J. Neurophysiol.*, vol.83, no.4, pp.2179–2191.
- [5] H. Adriansen et al., "Latencies of chemically evoked discharges in human cutaneous nociceptors and of concurrent subjective sensation," *Neurosci Lett*, vol.20, no.1, pp.55–59, 1980.
- [6] J. Van Hees et al., "C nociceptor activity in human nerve during painful and non painful skin stimulation," *J Neurol Neurosurg Psychiatry*, vol.44, no.7, pp.600–607, 1981.
- [7] P. Tanyaporn, et al., "A Human-inspired Pain Sensing System to Recognize Difference between Superficial and Deep Pain for Personal Care Robot Safety," 35th Annual Meeting of JCSS, pp.934–938, Aug., 2018.
- [8] C.S. Sherrington, "The Integrative Action of the Nervous System," (2nd ed., 1947), Yale University Press, New Haven, 1906.
- [9] D. Ruth et al., "Spatial summation of pressure pain: effect of body region," *Pain*, vol.106, no.3, pp.471–480, 2003.
- [10] National Institute of Advanced Industrial Science and Technology, "Digital human research group," <https://unit.aist.go.jp/hiri/dhrg/ja/dhdb/index.html>, accessed: Apr. 19, 2019. (Japanese).
- [11] M.A. Gibney et al., "Skin and subcutaneous adipose layer thickness in adults with diabetes at sites used for insulin injections: implications for needle length recommendations," *Curr Med Res Opin*, vol.26, no.6, pp.1519–1530, 2010.
- [12] J.T. Iivarinen et al., "Experimental and computational analysis of soft tissue stiffness in forearm using a manual indentation device," *Med Eng Phys*, vol.33, no.10, pp.1245–1253, 2011.
- [13] X. Liang et al., "Biomechanical Properties of in Vivo Human Skin from Dynamic Optical Coherence Elastography," *IEEE T BIO-MED ENG*, vol.57, no.4, pp.953–959, 2010.
- [14] C. Kerstyn et al., "A micromechanical model for the Young's modulus of adipose tissue," *Int J Solids Struct*, vol.47, no.21, pp.2982–2990, 2010.
- [15] A.S. Zil'bergelit et al., "Method of measuring the modulus of elasticity of human muscle tissue," *Biull Eksp Biol Med*, vol.96, no.12, pp.101–105, 1983.
- [16] J. Fridén et al., "Spastic muscle cells are shorter and stiffer than normal cells," *Muscle Nerve*, vol.27, no.2, pp.157–164, 2003.
- [17] H. Raviraj et al., "Insights into the effects of tensile and compressive loadings on human femur bone," *Adv Biomed Res*, vol. 3, no.101, 2014.
- [18] ISO15066, "Robots and robotic devices – Collaborative robots", 2016.
- [19] R. Polianskis et al., "Pressure-Pain Function in Desensitized and Hypersensitized Muscle and Skin Assessed by Cuff Algometry," *Pain*, vol.3, no.1, pp.28–37, 2002.
- [20] A.A. Fischer, "Pressure algometry over normal muscles: Standard values, validity and reproducibility of pressure threshold," *Pain*, vol.30, no.1, pp.115–126, 1987.
- [21] A.A. Fischer, "Pressure threshold meter: Its use for quantification of tender spots," *Arch Phys Med Rehabil*, vol.67, no.11, pp.836–838, 1986.
- [22] B. Jaeger, et al., "Quantification of changes in myofascial trigger point sensitivity with the pressure algometer following passive stretch," *Pain*, vol.27, no.2, pp.203–210, 1986.

### Information About the authors



Tanyaporn Pungrasmi プングラサミー タンヤポン  
Product Analysis Center  
プロダクト解析センター



Yusaku Shimaoka 島岡 優策  
Product Analysis Center  
プロダクト解析センター



Tamao Okamoto 岡本 球夫  
Ph.D. in Engineering  
Product Analysis Center  
プロダクト解析センター



Ryoji Watanabe 渡邊 竜司  
Product Analysis Center  
プロダクト解析センター